EXPERIMENTAL INVESTIGATIONS OF BEAM-BEAM INTERACTION IN STORAGE RINGS

V.L.Auslender, N.S.Dikansky, G.N.Kulipanov, S.I.Mishnev, S.G.Popov, Ju.A.Pupkov, A.N.Skrinsky, G.M.Tumaikin, Ju.M. Shatunov

Institute of Nuclear Physics, Siberian Department of the USSR Academy of Science, Novosibirsk, USSR

A. Beam-beam interaction effects at storing

On the VEPP-2 machine[1] the electron beam is stored with the 40–50 ma positron beam stored beforehand. A number of beam-beam interaction effects influencing both electron storing rate and positron life-time are to be suppressed.

1. As the electrons are stored at a comparatively low energy ($E \approx 200$ Mev) it is necessary to reduce the influence of noncoherent effects on beam damping. This is done through orbit splitting (orbit distance $2\Delta z \approx 4$ mm) in interaction regions with the help of an electric field. This makes it possible to store electrons up to 100 ma with no positron losses.

2. At the moment of injection the inflector excites oscillations of the whole stored electron beam, a part of it being lost presumably due to noncoherent beam-beam interaction. The part of the lost particles strongly depends upon injection energy, positron current and, though less, upon orbit splitting (Fig. 1).

3. The positron beam oscillation excitation by the coherently oscillating electron beam at the moment of injection is also possible. It is suppressed by the shifting of betatron frequencies by $\Delta\nu_z = 0.006$ with focusing electric field.

B. Noncoherent effects in the process of experiment

I. Beam density distribution

As the beam cross section in the VEPP-2 machine at energies more than 200 Mev is practically flat ($\Delta z \ll \Delta r$) beam-beam interaction brings about a change of density distribution in axial direction (Δz) whereas no change in radial direction was observed. The density distribution was measured with a dissector[2] and observed on the oscilloscope screen, the resolution of the system being 0.5 mm.

Typical oscillograms of density distribution in the axial direction when the beams collide are shown in Fig. 2a, b. (Fig. 2c is for the single beam case.) As a rule the size of only one beam changes (the weak one -- usually the positron beam). But if the size of the strong beam is increased by external excitation it will remain large even after the excitation is off. This state is unstable and may momentarily be reversed. The moment of transition depends upon the weak beam current.

Fig. 2 shows the following typical features of density distribution when the beams collide:

a) The central region of the beam has the density distribution close to the Gaussian though broader than in the case of a single beam.

b) When the betatron frequency is close to low resonant values there appear "wings" containing a significant part of the particles.

Fig. 3 shows the dependence of density in the beam center of VEPP-2 machine (in relative units) and the distribution "width" (containing 90% of particles) upon ν_z.

On the $e^- - e^-$ VEP-1 machine[1] the life-time of a 5 ma beam was measured depending upon the second beam current at the energy 135 Mev (Fig. 4). As beam life-time under these conditions is mainly defined by Ada-effect it characterizes the axial beam size. The beam-beam interaction effects bear an evidently resonant character being fully in accordance with theory[3]. Their influence can be essentially reduced by a correct choice of an operating point.

II. The influence upon luminosity

For the experiment on the VEPP-2 machine an operating point ($\nu_z = 0.8356$) was chosen with all the correcting elements being off. The "wings" at this operating point in energy range 290-440 Mev and at practically interesting current values were absent. The density distribution in weak beam was nearly Gaussian. The dependence of the axial size upon the strong beam current is shown in Fig. 5a.

Interaction effects reduce luminosity. It is especially convenient to consider specific luminosity connected only with the geometry of the interaction[4]

$$M = \frac{L}{I_+ I_-} = \frac{1}{e^2 f \cdot S_{eff}}$$

where L = luminosity

I_+, I_- = positron and electron currents respectively

e = electron charge

f = revolution frequency

s = effective beam cross-section for the Gaussian density distribution

$$(1)\quad S_{eff} = \frac{2\pi\sqrt{\sigma_z^{+2} + \sigma_r^{-2}} \cdot \sqrt{\sigma_z^{+2} + \sigma_z^{-2}}}{\eta} = \frac{4\pi\sigma_z}{\eta}\sqrt{\frac{\sigma_z^{+2} + \sigma_z^{-2}}{2}}$$

where σ_r^+, σ_z^+ and σ_r^-, σ_z^- mean squared dimensions of the positron and electron beams.

η = beam utilization coefficients depending upon the length of the interaction region.

The monitor for luminosity measurements is a small angle ($\alpha \sim 1^\circ$) elastic scattering[4]. Fig. 6 shows the dependence of $\eta = M_{max}\sigma_p$ upon energy at low currents when interaction effects may be neglected. Here σ_p = effective cross-section of monitor reactions. As $\sigma_p \sim E^{-2}$, the specific luminosity $M_{max} \sim E^{-3.2 \pm 0.5}$. At high currents the interaction effects reduce luminosity in accordance with Eq. 1. This is evident from Fig. 7, showing the dependence of $(\frac{M_{max}}{M})^2$ on $\Delta z_{1/2}^2$, where $\Delta z_{1/2}$ is the axial size of the weak beam measured by the dissector. Different slopes of lines are connected with a dependence of axial beam size at low current upon energy and a worse resolution of measuring devices. The deviation from Eq. 1 at high current may be explained by non-Gaussian density distribution.

As it has been mentioned above, the proper choice of the operating point provides for an essential reduction of the axial beam size growth. The change of betatron frequency with a decrease of electron current may prove to be useful (Fig. 8).

III. Interaction effects near low resonance ($\nu_z = \frac{5}{6}$)

Typical "wings" in density distribution of weak beam appear near low resonance. Fig. 9 shows that under certain conditions a larger part of particles is in the "wings". "Wings" filling time coincides on the order of magnitude with the scattering time on the residual gas for obtaining a given betatron oscillation amplitude.

References

1. E.A.ABRAMIAN et. al. Pros. of the Intern. Conf. on High Energy Accel. (DUBNA, 1963) p. 274.
2. V.L.AUSLENDER et. al. Pros. of the Intern. Symposium on Electron and Positron Storage Rings. (SACLAY, 1966) VII6-6.
3. Ia.S.DERBENEV et. al. Pros. of the Intern. Conf. on High Energy Accel. (FRASCATI, 1965) p. 375.
4. V.L.AUSLENDER et. al. Pros. of the Intern. Conf. on High Energy Accel. (FRASCATI, 1965).

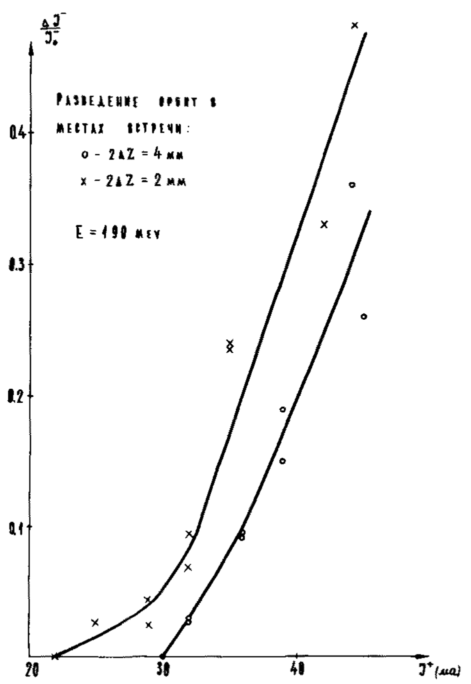

Fig. 1. The dependence of a part of lost electrons upon positron current at the moment of injection (VEPP-2).

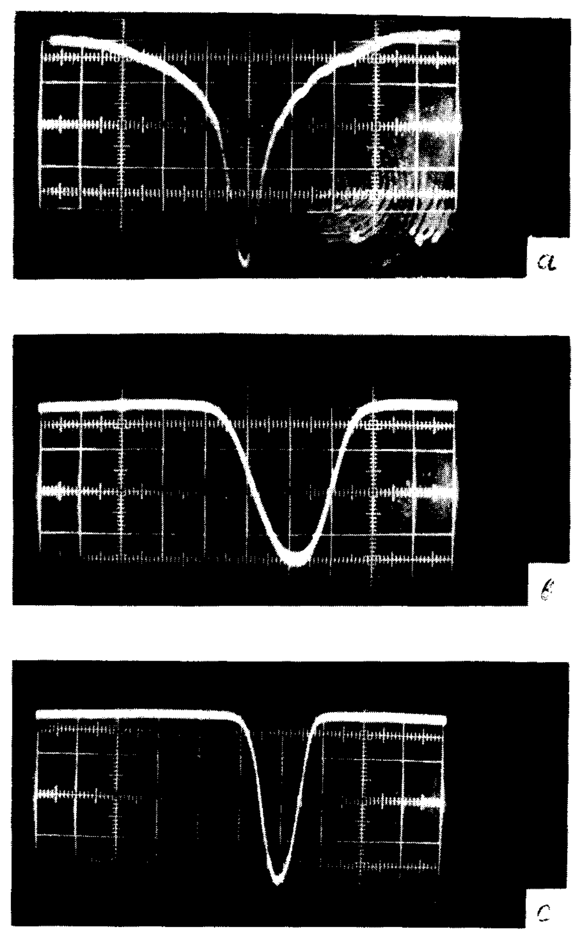

Fig. 2. The axial density distribution of positron beam.
a) ν_z = 0.8320 (near 5/6) } I_- = 15 ma
b) ν_z = 0.8356
c) ν_z = 0.8356 -- single beam

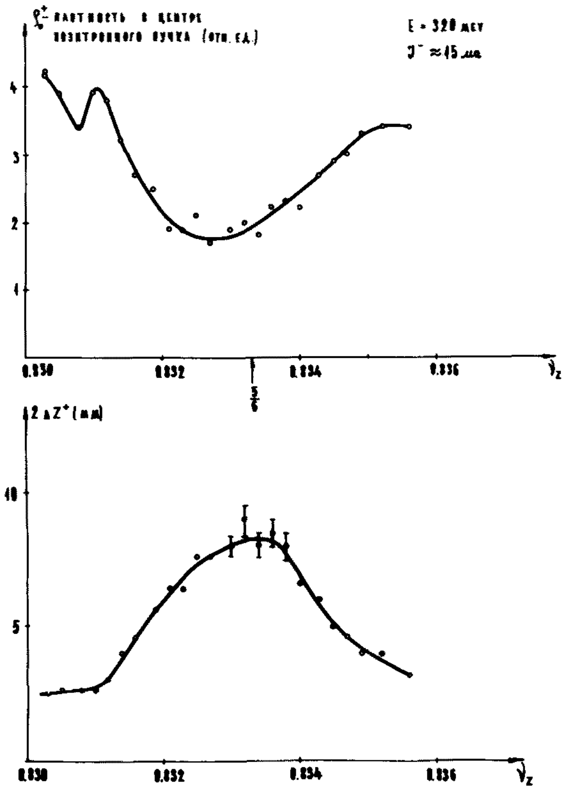

Fig. 3. Density in center of positron beam and "width" of density distribution depending on ν_z (VEPP-2).

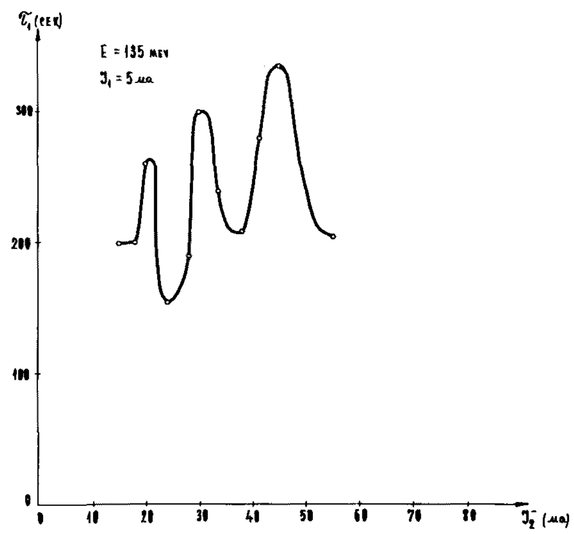

Fig. 4. Weak beam life-time depending upon strong beam current (VEPP-1).

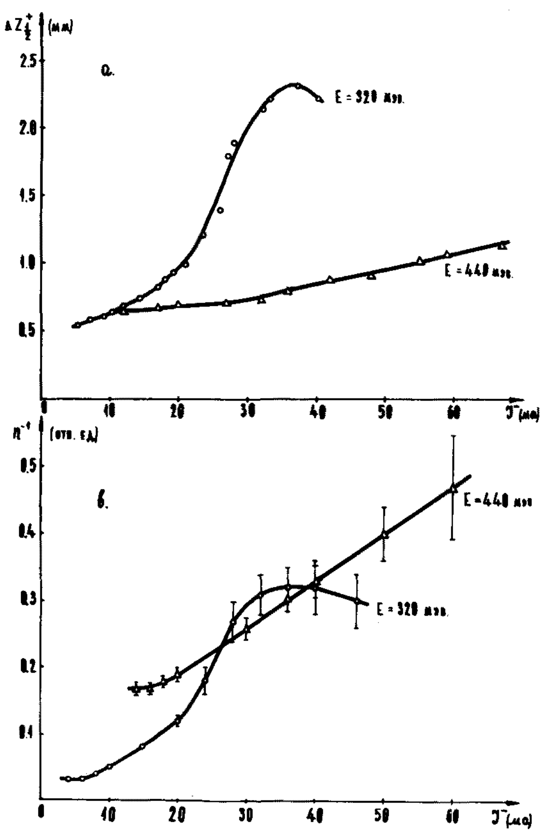

Fig. 5a. Weak beam axial size depending upon strong beam current.

Fig. 5b. Dependence of $n^{-1} = (M\sigma_p)^{-1}$ on strong beam current.

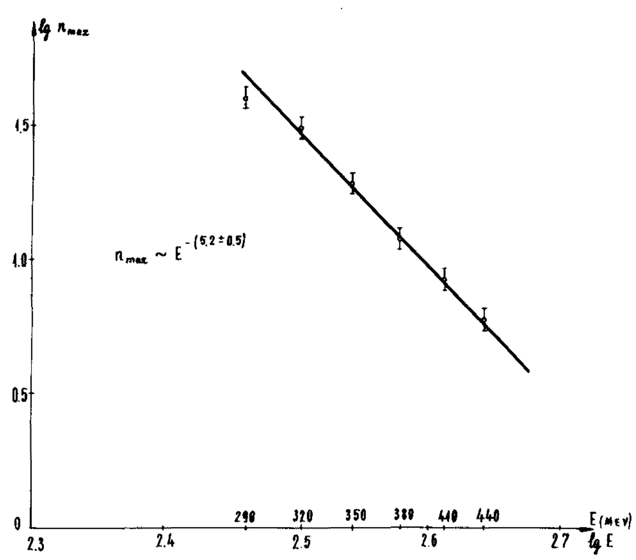

Fig. 6. Dependence of $n_{max} = M_{max}\sigma_p$ on energy at low current.

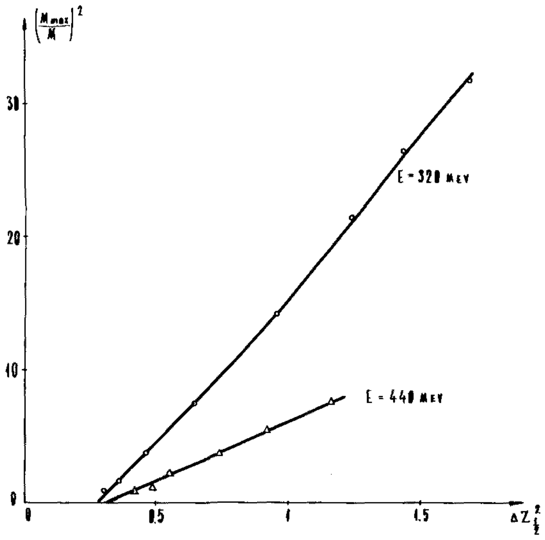

Fig. 7. Dependence of $(\frac{M_{max}}{M})^2$ on the weak beam axial size squared (VEPP-2).

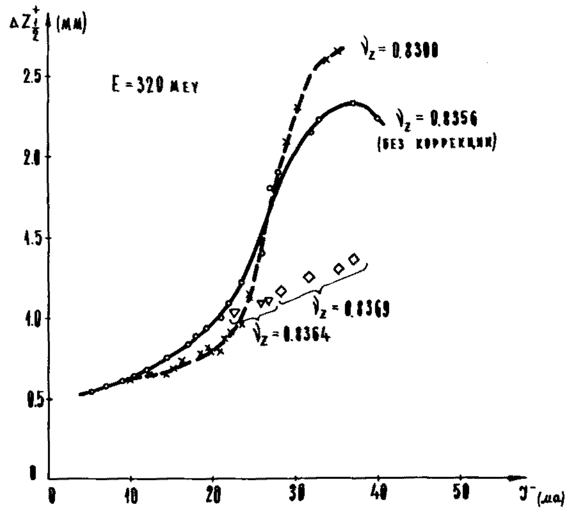

Fig. 8. Dependence of the weak beam axial size on the strong beam current with ν = correction (VEPP-2).

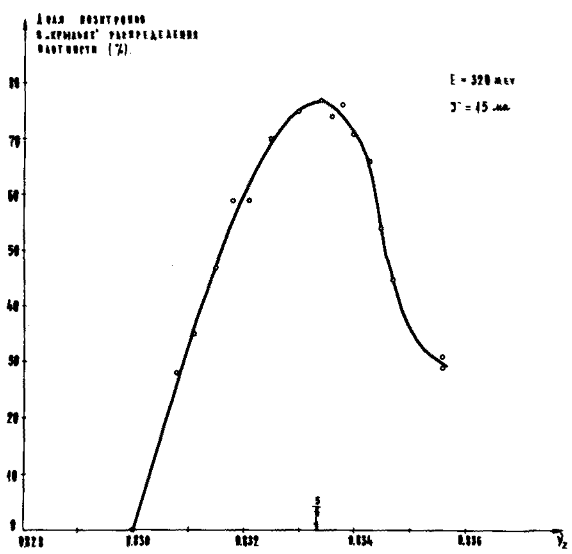

Fig. 9. Dependence of a part of weak beam particles filling the "wings" on ν_z.